Single-Post Inductive Obstacle in Rectangular Waveguide

YEHUDA LEVIATAN, MEMBER, IEEE, PING G. LI, ARLON T. ADAMS, SENIOR MEMBER, IEEE, AND JOSE PERINI, SENIOR MEMBER, IEEE

Abstract—**A rapidly converging moment solution for electromagnetic scattering by a single inductive post in a rectangular waveguide is obtained. The numerical results show good agreement with Marcuvitz's data as far as this data goes. Furthermore, Marcuvitz's curves are extended to cover data for large posts. This new data should allow one to design a simply constructed new type of narrow bandpass filter, namely, a filter consisting of large single posts. The successful use of this straightforward moment solution in solving the single-post problem suggests that this technique should prove useful in solving a variety of microwave discontinuities such as those involving thin or thick irises and posts of arbitrary shape.**

I. Introduction

IN DESIGNING bandpass filters for rectangular waveguides, one usually utilizes a number of sections, each of which comprises a high-Q resonant cavity. Such a cavity is formed of two obstacles nearly half a guide wavelength apart followed by a connecting length that is an odd multiple of a quarter-guide wavelength long. Of all conventional obstacles, a single cylindrical post, placed across the guide parallel to the narrow wall and parallel to the electric field of the dominant mode, is the most attractive from a fabrication point of view.

Schwinger had originally solved the single-post problem during World War II for small posts and his data is given in Marcuvitz's Waveguide Handbook [1]. One may think of the post problem simply in terms of the current which is induced on the post. Current is longitudinally directed (along the post axis) and varies circumferentially. The variation on each post may be represented by a Fourier series. Schwinger had taken into account the zeroth and first-order terms of the series. This had limited the results to posts which were of moderate size and were distant from the walls and from each other. Those interested in microwave filter design soon found out that when narrow bandpass filters were desired they needed larger posts. Mariani [2] recognized the need for larger posts, but, because data was lacking, decided to analyze the triple-post configuration consisting of three small posts, each within the range of Schwinger's analysis. Also available is a work by Bradshaw [3] who derived improved variational expressions for scattering from a round metal post with gap.

This paper develops a moment solution [4] for the single-post problem and extends Marcuvitz's curves to cover data for large posts. This new data should allow one to design a simply constructed new type of narrow bandpass filter, namely, a filter consisting of large single posts.

In treating the single-post problem, we use a multifilament representation of the current. The field due to each filament is then expanded in terms of waveguide modes. This leads to a slowly converging series which is not convenient for computation. Fortunately, this severe drawback can be overcome by converting the series to a rapidly converging one. Subsequently, a multiple point-matching of the boundary condition is applied and the unknown filamentary currents are readily obtained. Finally, we calculate the scattering matrix for the post two-port junction, and then obtain the equivalent T network for that junction. We also use the unitary condition of the scattering matrix, which is equivalent to the power conservation law, to estimate how good our approximate solution is.

In addition, we employ another independent method of moment procedure to provide a check against the first one in regions where no experimental data or other analytical results are available. The other method uses a multipole representation of the current and a Galerkin procedure for the boundary condition. The method uses an infinite series of images rather than the waveguide-mode representation, and we found a way of summing the series analytically. A detailed analysis of the second method will appear in a forthcoming paper.

The computer results for the single post from the two dissimilar methods agree with each other within a fraction of one percent and plot right on top of Marcuvitz's data as far as this data goes. Furthermore, we extend Marcuvitz's curves to cover data for large posts. The results obtained from both methods for large posts also show a remarkable agreement. Apparently these methods both can provide an accurate solution. It also appears likely that the first method can be applied to other classes of problems such as those involving thin or thick irises and posts of arbitrary shape.

II. Problem Specification and Equivalent Situation

The physical configuration of the problem under study is shown in Fig. 1, together with the coordinate system used.

Manuscript received November 22, 1982; revised April 26, 1983.

The authors are with the Department of Electrical and Computer Engineering, Syracuse University, Syracuse, NY 13210.

0018-9480/83/1000-0806$01.00 ©1983 IEEE

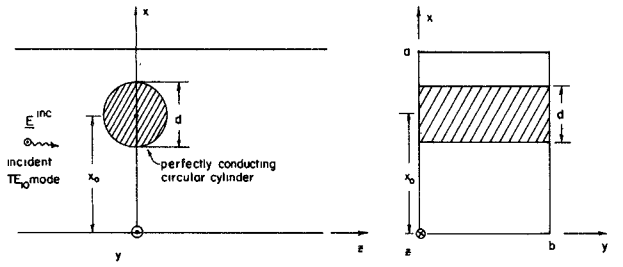

Fig. 1. Perfectly conducting circular inductive post in rectangular waveguide.

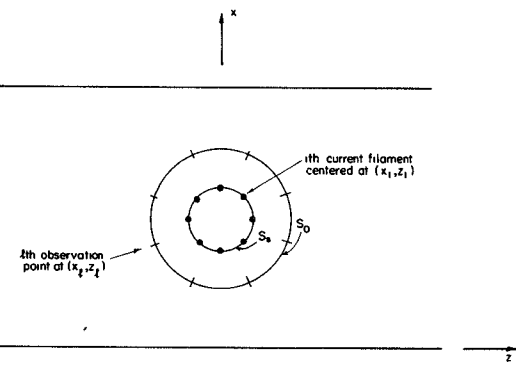

Fig. 2. Equivalent current filaments used to replace the conducting post surface.

Here, we consider a perfectly conducting circular post of diameter d centered at $x = x_0$, $z = 0$ in a cylindrical waveguide of rectangular cross section. The width of the rectangular guide is a and its height is b. The waveguide is filled with homogeneous medium of constitutive parameters μ and ϵ. We are not accounting for dissipation and thus μ and ϵ are considered real. It is assumed that the incident wave is the dominant mode, namely, the TE_{10} mode, traveling in the positive z-direction, with $\exp(j\omega t)$ time dependence. Since the incident wave does not vary in the y-direction and the properties of the post are uniform along the y-direction, the total field in the rectangular waveguide does not vary in the y-direction and reduces to a two-dimensional one. Our objective is to represent the scattered field in terms of waveguide modes, thereby readily obtaining the scattering matrix of the system.

In order to find the scattered field in the waveguide, we replace the perfectly conducting circular surface S_0 by a current distribution J placed on a suitably chosen cylindrical surface of circular cross section S_s, taken to be either the same as S_0 or, with a view toward obtaining improved numerical solution [5], concentric and inside S_0. This current is assumed to radiate in the waveguide with the post absent. The electric field in the waveguide, denoted by $\boldsymbol{E}$, is

$$\boldsymbol{E} = \boldsymbol{E}(\boldsymbol{J}) + \boldsymbol{E}^{\text{inc}} \tag{1}$$

where $\boldsymbol{E}(\boldsymbol{J})$ is the electric field due to the equivalent current $\boldsymbol{J}$, and $\boldsymbol{E}^{\text{inc}}$ is the electric field of the incident TE_{10} mode, both calculated with the post absent. If $\boldsymbol{J}$ were chosen such that the tangential component of $\boldsymbol{E}$ vanished on S_0, then $\boldsymbol{E}(\boldsymbol{J})$ would strictly be the field scattered by the post on and external to S_0 in the original problem. Unfortunately, the task to find this $\boldsymbol{J}$ can be considerably complicated.

While analytical headway can be gained only at the expense of a more cumbersome formulation, acceptably accurate results may be obtained from an approximate numerical solution without seriously taxing the computing system. To obtain an approximate solution, it is convenient to place N y-directed current filaments I_i, $i = 1, \cdots, N$ equally spaced on S_s, where $I_1, I_2, \cdots, I_N$ are constants yet to be determined, as depicted in Fig. 2, and impose the boundary condition with regard to the component of $\boldsymbol{E}$ tangential to the post surface at a selected number of points, equal to the number of sources N, equally spaced on S_0. This, briefly discussed, process of solving the problem will become apparent in the forthcoming section.

III. Formulation of the Problem

First, we need to derive the field due to the ith y-directed current filament $\boldsymbol{J}_i$ given by

$$\boldsymbol{J}_i = \boldsymbol{u}_y J_{iy} = \boldsymbol{u}_y I_i \delta(x - x_i) \tag{2}$$

situated over the $z = z_i$ cross section of the waveguide. In (2), $\boldsymbol{u}_y$ is a unit vector in the y-direction and the δ denotes the Dirac delta function. Since the current in (2) is y-directed, we expect that a y-directed magnetic vector potential $\boldsymbol{A}_i$ is sufficient for representing the field [6]. Also, because $\boldsymbol{J}_i$ is independent of the spatial y direction, so is $\boldsymbol{A}_i$. Further, for an analysis of transmission characteristics, an expression in terms of waveguide modes is most suitable. It then follows that

$$\boldsymbol{A}_i = \boldsymbol{u}_y \psi_i = \boldsymbol{u}_y \sum_{m=1}^{\infty} B_{im} \sin \frac{m\pi x}{a} e^{-jk_{zm}|z - z_i|}. \tag{3}$$

In (3), the k_{zm} are modal wavenumbers given by

$$k_{z1} = \sqrt{k^2 - \left(\frac{\pi}{a}\right)^2} \tag{4}$$

$$k_{zm} = -j\sqrt{\left(\frac{m\pi}{a}\right)^2 - k^2}, \qquad m \neq 1 \tag{5}$$

where $k = \omega\sqrt{\mu\epsilon}$ is the wavenumber in the waveguide region, and B_{im} are coefficients given by

$$B_{im} = \frac{1}{jk_{zm}a} I_i \sin \frac{m\pi x_i}{a}. \tag{6}$$

Finally, the components of the electric field are derived from (3). As expected, the electric field has only a y component given by

$$E_{iy} = -\frac{k\eta I_i}{a} \sum_{m=1}^{\infty} \frac{1}{k_{zm}} \sin \frac{m\pi x_i}{a} \sin \frac{m\pi x}{a} e^{-jk_{zm}|z - z_i|} \tag{7}$$

where $\eta = \sqrt{\mu/\epsilon}$ is the intrinsic impedance of the medium filling the waveguide.

Unfortunately, the series in (7) converges slowly and is not convenient for computation. To convert it to a more

rapidly converging one, we introduce the auxiliary series

$$S_i^{\text{aux}} = -\frac{k\eta I_i}{a}\sum_{m=1}^{\infty}\frac{1}{\frac{m\pi}{a}}\sin\frac{m\pi x_i}{a}\sin\frac{m\pi x}{a}e^{-(m\pi/a)|z-z_i|} \tag{8}$$

which, when summed in closed form, reduces to (Appendix)

$$S_i^{\text{aux}} = -\frac{k\eta I_i}{2\pi}\operatorname{Re}\left\{\ln\left[\frac{1-e^{j(\pi/a)(|x+x_i|+j|z-z_i|)}}{1-e^{j(\pi/a)(|x-x_i|+j|z-z_i|)}}\right]\right\}. \tag{9}$$

Note that for large m, the terms of the series in (7) approach those of S_i^{aux}. Furthermore, subtracting (8) from (7) and adding the resultant expression into (9), we obtain

$$E_{iy} = S_i^{\text{aux}} + S_i \tag{10}$$

where S_i^{aux} is given by (9) and S_i is the rapidly convergent summation

$$S_i = -\frac{k\eta I_i}{a}\sum_{m=1}^{\infty}\left(\frac{e^{-jk_{zm}|z-z_i|}}{k_{zm}} - \frac{e^{-(m\pi/a)|z-z_i|}}{\frac{m\pi}{a}}\right)\cdot\sin\frac{m\pi x_i}{a}\sin\frac{m\pi x}{a}. \tag{11}$$

This completes evaluation of the field at observation point (x, z) due to current filament I_i situated at (x_i, z_i). The result represents the Green's function for a line current in a rectangular guide in terms of a rapidly converging series of waveguide modes.

Referring now to (1), we need know $\boldsymbol{E}(\boldsymbol{J})$ for the N y-directed current filaments. In view of the preceding discussion, this field is

$$\boldsymbol{E}(\boldsymbol{J}) = \boldsymbol{u}_y\sum_{i=1}^{N}E_{iy}. \tag{12}$$

The incident field should also be specified. For the dominant TE_{10} mode, this field is

$$\boldsymbol{E}^{\text{inc}} = \boldsymbol{u}_y E^{\text{inc}} = \boldsymbol{u}_y\sin\frac{\pi x}{a}e^{-jk_{z1}z}. \tag{13}$$

Next, (12) and (13) are substituted into (1), and the boundary condition is simultaneously imposed at N points (x_l, z_l), $l = 1, 2, \cdots, N$. This reduces the functional equation (1) to a matrix form in which the various matrices are interpreted in terms of generalized network parameters. We have

$$[Z_g]\vec{I} = \vec{V}^i. \tag{14}$$

In (14), $[Z_g]$ is a square matrix of order N called the generalized impedance whose (i, l) element is the field due to the ith current filament E_{iy} at observation point (x_l, z_l). The subscript "g" is used to make the generalized impedance matrix of (14) and a two-port network impedance matrix to be introduced in Section IV distinct. $\vec{I}$ is an N-element column vector called the generalized unknown current whose ith element is I_i. $\vec{V}^i$ is an N-element column vector called the generalized voltage source whose lth element is the negative of E^{inc} at observation point (x_l, z_l). Finally, if $[Z_g]$ is not singular, the unknown current vector is readily given by

$$\vec{I} = [Z_g]^{-1}\vec{V}^i \tag{15}$$

where $[Z_g]^{-1}$ denotes the inverse of $[Z_g]$.

IV. Scattering Matrix and Equivalent Circuit

Once the unknown current vector is obtained from (15), the scattered field in the waveguide can be readily computed. We consider two reference planes T_1 and T_2 placed, respectively, on $z = z_{T1}$ and $z = z_{T2}$ far from the cylinder axis such that

$$z_{T1} \ll \min(z_i, \quad i = 1, \cdots, N) \tag{16}$$

$$z_{T2} \gg \max(z_i, \quad i = 1, \cdots, N). \tag{17}$$

From (16) and (17), one easily recognizes that

$$|z_{T1} - z_i| = z_i - z_{T1}, \quad i = 1, \cdots, N \tag{18}$$

$$|z_{T2} - z_i| = z_{T2} - z_i, \quad i = 1, \cdots, N. \tag{19}$$

In addition, it is assumed that the distance to each of the planes T_1 and T_2 from the cylinder axis is an integral multiple of the guide wavelength so that

$$e^{\pm jk_{z1}z_{T1}} = e^{\pm jk_{z1}z_{T2}} = 1. \tag{20}$$

It is noteworthy that because terminal planes T_1 and T_2 are located an integral multiple of the guide wavelength away from the $z = 0$ plane, the scattering matrix for these planes is identical to the scattering matrix for terminal planes $z = 0^-$ and $z = 0^+$. Clearly, the only propagating mode is the dominant TE_{10} ($m = 1$) mode. It then follows from (7) and (12) on use of (18)–(19) that the scattered field at T_1 and T_2 is

$$\boldsymbol{E}^S|_{T_1} = \boldsymbol{u}_y E_y^S|_{T_1} = \boldsymbol{u}_y\sum_{i=1}^{N} -\frac{k\eta I_i}{k_{z1}a}\sin\frac{\pi x_i}{a}\sin\frac{\pi x}{a}e^{-jk_{z1}(z_i - z_{T1})} \tag{21}$$

$$\boldsymbol{E}^S|_{T_2} = \boldsymbol{u}_y E_y^S|_{T_2} = \boldsymbol{u}_y\sum_{i=1}^{N} -\frac{k\eta I_i}{k_{z1}a}\sin\frac{\pi x_i}{a}\sin\frac{\pi x}{a}e^{-jk_{z1}(z_{T2} - z_i)}. \tag{22}$$

The incident field is given by (13). At T_1 and T_2, this field is

$$\boldsymbol{E}^{\text{inc}}|_{T_1} = \boldsymbol{u}_y E_y^{\text{inc}}|_{T_1} = \boldsymbol{u}_y\sin\frac{\pi x}{a}e^{-jk_{z1}z_{T1}} \tag{23}$$

$$\boldsymbol{E}^{\text{inc}}|_{T_2} = \boldsymbol{u}_y E_y^{\text{inc}}|_{T_2} = \boldsymbol{u}_y\sin\frac{\pi x}{a}e^{-jk_{z1}z_{T2}}. \tag{24}$$

Next, we use (21)–(24) to express the elements S_{11} and S_{21} of the scattering matrix $[S]$. Here, S_{11}, the reflection coefficient at T_1, is given by

$$S_{11} = \frac{E_y^S|_{T_1}}{E_y^{\text{inc}}|_{T_1}} \tag{25}$$

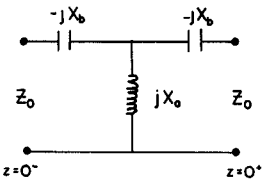

Fig. 3. Typical equivalent circuit for circular inductive post.

and S_{21}, the transmission coefficient at T_2, is given by

$$S_{21} = \frac{\left(E_y^{\text{inc}} + E_y^S\right)|_{T_2}}{E_y^{\text{inc}}|_{T_1}}. \tag{26}$$

Applying (20) in (21)–(24) and subsequently substituting the resultant equations into (25) and (26), we obtain

$$S_{11} = \sum_{i=1}^{N} -\frac{k\eta I_i}{k_{z1}a} \sin\frac{\pi x_i}{a} e^{-jk_{z1}z_i} \tag{27}$$

$$S_{21} = 1 + \sum_{i=1}^{N} -\frac{k\eta I_i}{k_{z1}a} \sin\frac{\pi x_i}{a} e^{jk_{z1}z_i}. \tag{28}$$

The remaining elements S_{12} and S_{22} can be found from reciprocity and symmetry considerations, respectively. It follows that

$$S_{12} = S_{21} \tag{29}$$

$$S_{22} = S_{11}. \tag{30}$$

This completes evaluation of the elements of the scattering matrix for terminal planes $z = 0^-$ and $z = 0^+$.

We wish now to obtain an equivalent circuit for the circular inductive post. A typical two-port circuit representation of this obstacle is the T network shown in Fig. 3. To obtain the T network parameters, we first express the normalized elements of impedance matrix $[Z]$ of the junction in terms of the scattering matrix parameters. The matrix relation between the scattering and impedance matrices is given in [6]. This relation is readily expressed as

$$\frac{1}{Z_0}[Z] = -([S]+[U])([S]-[U])^{-1} \tag{31}$$

where $[U]$ is the unit matrix and $Z_0 = \omega\mu/k_{z1}$ is the characteristic impedance of the propagating mode. It then follows that

$$\frac{Z_{11}}{Z_0} = \frac{(1+S_{11})(1-S_{22})+S_{12}S_{21}}{(1-S_{11})(1-S_{22})-S_{12}S_{21}} \tag{32}$$

$$\frac{Z_{12}}{Z_0} = \frac{2S_{12}}{(1-S_{11})(1-S_{22})-S_{12}S_{21}} \tag{33}$$

$$\frac{Z_{21}}{Z_0} = \frac{2S_{21}}{(1-S_{11})(1-S_{22})-S_{12}S_{21}} \tag{34}$$

$$\frac{Z_{22}}{Z_0} = \frac{(1-S_{11})(1+S_{22})+S_{12}S_{21}}{(1-S_{11})(1-S_{22})-S_{12}S_{21}}. \tag{35}$$

Finally, the normalized parameters of the equivalent circuit are computed. We have

$$j\frac{X_a}{Z_0} = \frac{Z_{12}}{Z_0} = \frac{2S_{21}}{(1-S_{11})^2 - S_{21}^2} \tag{36}$$

$$-j\frac{X_b}{Z_0} = \frac{Z_{11}-Z_{12}}{Z_0} = \frac{1+S_{11}-S_{21}}{1-S_{11}+S_{21}}. \tag{37}$$

V. Numerical Results

A computer program using the preceding formulation has been written to calculate the normalized components of the equivalent circuit for the circular inductive post. This program is described and listed in [7]. It should be emphasized that although this program is applicable exclusively to the single-post obstacle, it can be generalized in a straightforward manner to encompass other y-independent obstacles. Some computational results obtained with this program are given in this section.

The question of appropriately choosing the circular surface S_s and the number of filaments N arises naturally. Studies have shown that the rate of convergence of the results is independent of the choice of S_s. The phenomenon is linked to the fact that the average spacing in the z-direction between observation and field points, which determines how rapidly the nonpropagating modes are attenuated, is actually unchanged. Note that although the following curves pertain specifically to the case in which r_s/r_0, the ratio between the radius of S_s and the radius of S_0 is one, other ratios were also considered. Some examples are $r_s/r_0 = 0.1$, $r_s/r_0 = 0.5$, and $r_s/r_0 = 0.8$. In all four cases, the rates of convergence as well as the results were virtually identical.

The above reasoning is also helpful in understanding why the rate of convergence is, with one exception, insensitive to a circumferential shift of equivalent source points relative to observation points. The exception is when this circumferential shift is half the angular distance between two adjacent observation points. In this case, due to symmetry, the general impedance matrix becomes singular. With regard to N, even for choices less than optimal, acceptably accurate results are obtained. As a rule of thumb, one may choose 20 sources per one wavelength circumference.

Attention should also be recalled to the summation in (11). As a practical necessity, a truncation of the infinite series is required. The truncation causes a deviation from the correct solution. Fortunately, this error can be quantitatively estimated from the unitary condition of the scattering matrix, which is equivalent to the power conservation law [8]

$$|S_{11}|^2 + |S_{21}|^2 = 1. \tag{38}$$

In the cases under consideration, (38) has been satisfied with a less than 0.1-percent error.

Fig. 4 exhibits normalized reactances $(X_a/Z_0)(\lambda_g/2a)$ and $(X_b/Z_0)(\lambda_g/2a)$ as a function of d/a for centered

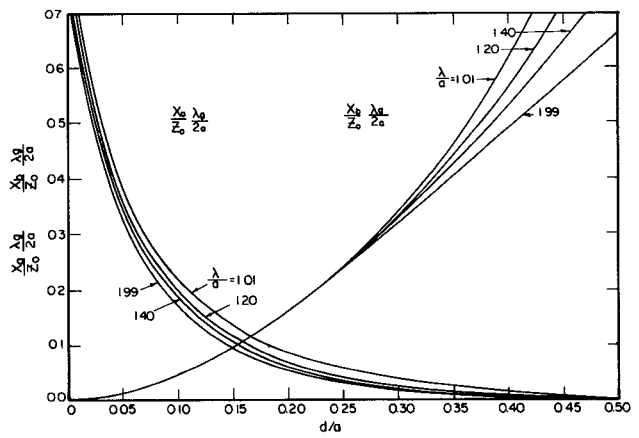

Fig. 4. Circuit parameters for centered ($x_0 = 0.5a$) inductive post in rectangular guide.

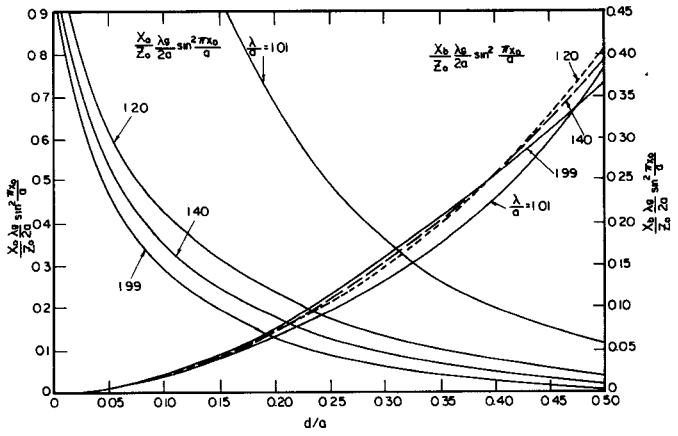

Fig. 5. Circuit parameters for off-centered ($x_0 = 0.3a$) inductive post in rectangular guide.

post ($x_0 = 0.5$a) for various frequencies. Here, $\lambda_g = 2\pi/k_{z1}$ is the wavelength of the TE_{10} mode. Cases shown are $\lambda/a = 1.01$, $\lambda/a = 1.20$, $\lambda/a = 1.40$, and $\lambda/a = 1.99$, where $\lambda = 2\pi/k$ is the wavelength in the medium filling the waveguide. One should note that the graphs for $\lambda/a = 1.01$ describe the case in which the frequency is just below the cutoff frequency of the TE_{20} mode. Likewise, the graphs for $\lambda/a = 1.99$ describe the case in which the frequency is just above the cutoff frequency of the TE_{10} mode. The results have been checked against those of Marcuvitz [1] and they plot right on top of Marcuvitz's data as far as this data goes, i.e., for $d/a < 0.25$. It is interesting to view that a dispersion of the $(X_b/Z_0)(\lambda_g/2a)$ curve occurs when $d/a > 0.25$. Although we had always assumed that Marcuvitz's data was accurate, it is indeed remarkable that the limit of validity he stated for the approximate frequency independent curve $X_b/Z_0\lambda_g/2a$ was $d/a = 0.25$.

Fig. 5 presents normalized reactances $(X_a/Z_0)(\lambda_g/2a)\sin^2(\pi x_0/a)$ and $(X_b/Z_0)(\lambda_g/2a)\sin^2(\pi x_0/a)$ as a function of d/a for off-centered post ($x_0 = 0.3a$) for various frequencies. Cases shown are, again, $\lambda/a = 1.01$, $\lambda/a = 1.20$, $\lambda/a = 1.40$, and $\lambda/a = 1.99$. The $(X_a/Z_0)(\lambda_g/2a)\sin^2(\pi x_0/a)$ curve seems to disperse at $d/a = 0.075$ and indicates that the range within which the Marcuvitz's frequency independent curve is valid is actually smaller. This difference probably can be attributed to the fact that when the post is closer to one of the waveguide walls, higher order terms are needed for the Fourier series representation in Schwinger's analysis.

VI. Discussion

The problem of a single inductive post in a rectangular waveguide has been formulated in terms of an equivalent electric current. The operator equation for the equivalent current has been reduced to a matrix equation by using multifilament representation of the current and point-matching of the boundary condition. The Green's function for a current filament in rectangular waveguide has been expanded in terms of waveguide modes and subsequently converted to a rapidly converging series. Applying the improved Green's function in a moment solution, we have obtained the currents. These currents have then been applied to derive the scattering matrix and the equivalent T network for the post junction.

The computed results show good agreement with Marcuvitz's data as far as this data goes. The technique has also been applied to posts of large diameter. In view of the lack of experimental data or other analytical results for large posts, we have pursued another independent method of moment procedure to provide a check against the first one. The results from both methods have shown a remarkable agreement with each other within a fraction of one percent.

It should be emphasized that the accuracies achievable by these theoretical models are excellent with respect to any engineering needs, particularly since additional contributions to the fields arise due to losses at the conducting surfaces and due to scattering from rough surfaces or material inhomogeneities. Both theoretical methods for achieving the parameters of the equivalent circuit should, therefore, be viewed as very good ones throughout the entire range $0 \leqslant d/a \leqslant 1$. Note, however, that we have limited the data displayed to $d/a \leqslant 0.5$. This was done because posts in the range $d/a > 0.5$ would yield extremely high-Q filters which are not commonly encountered in practice.

The new data presented here should allow one to design a simply constructed new type of narrow bandpass filter, namely, a filter consisting of large single posts. Moreover, the successful use of a simple moment approach together with the rapidly converging Green's function in solving the single-post problem suggests that this technique should prove useful in solving a variety of microwave discontinuities such as those involving thin or thick irises and posts of arbitrary shape. Specifically, an extension to treat arrays of posts appears to be fairly straightforward.

Appendix
Summation Formula for S_t^{aux}

In this Appendix, the series S_t^{aux} given by (8) is summed in closed form.

First, consider the series

$$Q_{\pm} = \sum_{m=1}^{\infty} \frac{e^{jm(\bar{x}_{\pm}+j\bar{z})}}{m}. \tag{A1}$$

Here, $\bar{x}_{\pm} = \pi/a|x \pm x_i|$ and $\bar{z} = \pi/a|z - z_i|$. Moreover, we confine ourselves to $0 \leqslant \bar{x}_{\pm} < 2\pi$, $\bar{z} \geqslant 0$, and exclude the case in which both $\bar{x}_{\pm}$ and $\bar{z}$ are zero. A summation formula for $Q_{\pm}$ is obtainable straightforwardly from the Taylor expansion of

$$f(w) = -\ln(1+w) \tag{A2}$$

about $w = 0$. For $|w| \leqslant 1$, with $w = -1$ excluded, we have

$$f(w) = -\ln(1+w) = -w + \frac{w^2}{2} - \frac{w^3}{3} + \cdots + (-1)^m \frac{w^m}{m} + \cdots. \tag{A3}$$

Setting

$$w = -e^{j(\bar{x}+j\bar{z})} \tag{A4}$$

one can readily verify that the requirements stated with regard to w are satisfied. Now, substituting (A4) into (A3), we arrive at

$$\sum_{m=1}^{\infty} \frac{e^{jm(\bar{x}+j\bar{z})}}{m} = -\ln(1 - e^{j(\bar{x}+j\bar{z})}). \tag{A5}$$

Subsequently, we equate the real part of each side of (A4). That is

$$\sum_{m=1}^{\infty} \frac{1}{m} \cos m\bar{x}_{\pm} e^{-m\bar{z}} = \mathrm{Re}\left\{\ln\left[\frac{1}{1 - e^{j(\bar{x}_{\pm}+j\bar{z})}}\right]\right\}. \tag{A6}$$

We turn now to S_i^{aux} as given by (8). Applying straightforward algebraic reduction, we obtain

$$S_i^{\mathrm{aux}} = -\frac{k\eta I_i}{2\pi}\left[\sum_{m=1}^{\infty} \frac{1}{m} \cos m\bar{x}_{-} e^{-m\bar{z}} - \sum_{m=1}^{\infty} \frac{1}{m} \cos m\bar{x}_{+} e^{-m\bar{z}}\right]. \tag{A7}$$

Then, in view of (A6), we are led to

$$S_i^{\mathrm{aux}} = -\frac{k\eta I_i}{2\pi} \mathrm{Re}\left\{\ln\left[\frac{1 - e^{j(\bar{x}_{+}+j\bar{z})}}{1 - e^{j(\bar{x}_{-}+j\bar{z})}}\right]\right\}. \tag{A8}$$

Finally, substituting $\bar{x}_{+}$, $\bar{x}_{-}$, and $\bar{z}$ into (A8) one readily obtains the summation formula given by (9).

References

[1] N. Marcuvitz, Ed., *Waveguide Handbook*, M.I.T. Rad. Lab. Ser., vol. 10. New York: McGraw-Hill, 1951, pp. 257–262.

[2] E. A. Mariani, "Design of narrow-band, direct-coupled waveguide filters using triple-post inductive obstacles," United States Army Electronics Command, Fort Monmouth, NJ, Tech. Rep. ECON-2566, Mar. 1965.

[3] J. A. Bradshaw, "Scattering from a round metal post and gap," *IEEE Trans. Microwave Theory Tech.*, vol. MTT-21, pp. 313–322, May 1973.

[4] R. F. Harrington, *Field Computation by Moment Methods*. New York: Macmillan, 1968.

[5] R. S. Popovidi and Z. S. Tsverikmazashvili, "Numerical study of a diffraction problem by a modified method of non-orthogonal series," *U.S.S.R. Computational Mathematics and Mathematical Physics*, vol. 17, no. 2, pp. 93–103, 1977.

[6] R. E. Collin, *Field Theory of Guided Waves*. New York: McGraw-Hill, 1960.

[7] Y. Leviatan *et al.*, "Single-post inductive obstacle in rectangular waveguide," Dept. Elec. and Comput. Eng., Syracuse Univ., Tech. Rep. TR-82-13, Nov. 1982.

[8] N. Okamoto, I. Nishioka, and Y. Nakanishi, "Scattering by a ferrimagnetic circular cylinder in a rectangular waveguide," *IEEE Trans. Microwave Theory Tech.*, vol. MTT-19, pp. 521–527, June 1971.

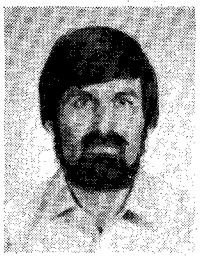

Yehuda Leviatan (S'81–M'82) was born in Jerusalem, Israel, on September 19, 1951. He received the B.Sc. and M.Sc. degrees in electrical engineering from the Technion–Israel Institute of Technology, Haifa, Israel, in 1977 and 1979, respectively, and the Ph.D. degree in electrical engineering from Syracuse University, Syracuse, NY, in 1982.

He held a Teaching Assistantship during his graduate work from 1977 to 1979 at the Technion, a Research Assistantship during his graduate work from 1979 to 1981 at Syracuse University, and a Postdoctoral Research position at Syracuse University during the summer of 1982. From 1980–1982 he was also engaged as a part-time Research Engineer at the Syracuse Research Corporation. In September 1982 he joined the Faculty of the Electrical and Computer Engineering Department at Syracuse University as an Assistant Professor. He provides consulting services to the Syracuse Research Corporation and to IBM. His research interests are in the areas of mathematical and numerical methods applied to antennas, transmission lines, and waveguides, scattering and transmission through apertures, near fields of radiating systems, and adaptive arrays.

Ping Guan Li was born in 1945 in Changle County, Fukien Province, China. He graduated from the Department of Radio-Electronics, Tsinghua University, People's Republic of China, in February 1968. He came to the United States in 1981 for postgraduate studies at Syracuse University where he received the M.S. degree in 1982. He is now working toward the Ph.D. degree under the guidance of Professor A. T. Adams of Syracuse University.

Arlon T. Adams (M'58–SM'72) received the B.A. degree in applied science from Harvard University, Cambridge, MA in 1953, and the M.S. and Ph.D. degrees in electrical engineering in 1961 and 1964, respectively, both from the University of Michigan, Ann Arbor.

He served as a Line Officer in the Atlantic Destroyer Fleet from 1953 to 1957, and until 1959 he was employed by Sperry Gyroscope Company, Long Island, NY. From 1959 to 1963 he was a Graduate Research Associate at the University of Michigan, Ann Arbor. In 1963 he joined the Faculty of Syracuse University, Syracuse, NY, where he is presently Professor of Electrical Engineering. During the academic year 1976–1977, he was a Visiting Scholar at the University of California at Berkeley where he worked on infrared antennas. His current interests are in numerical methods for electromagnetic problems. He is the author of a textbook on electromagnetic theory, coauthor of a textbook on electromagnetic compatibility, and has published over 70 papers on electromagnetics.

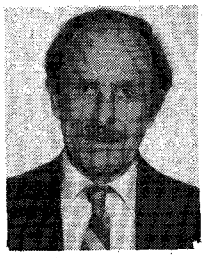

Jose Perini (M'61–SM'76) was born in São Paulo, Brazil. He received the B.S. degree in electrical and mechanical engineering from Escola Politecnica de São Paulo, São Paulo, Brazil, in 1952.

Subsequently, he worked for Real Transportes Aeroes, a Brazilian airline company, for three years, as Manager for Radio Maintenance, and in the last six months, as Assistant to the Manager of General Maintenance. In 1955 he joined the Electrical Engineering Department of Escola Politecnica de São Paulo, as an Assistant Professor, teaching until 1958. During this time, he also conducted ionospheric research. He received the Ph.D. degree in electrical engineering from Syracuse University, Syracuse, NY, in 1961. From 1959 to 1961, while studying at Syracuse, he was also a consultant for General Electric (G.E.) Co. in the Television Transmitting Antenna area. His Ph.D. dissertation was derived from this work. In 1961 he returned to Brazil as an Associate Professor of Electrical Engineering at Escola Politecnica de Sao Paulo and also as a consultant for G.E. of Brazil. In September 1962 he became Assistant Professor of Electrical Engineering at Syracuse University, where he was promoted to Associate Professor in 1966 and to Professor in 1971. He rejoined G.E. in Syracuse as a consultant in the same area of TV transmitting antennas until 1969. He has had many research contracts with the Navy, Air Force, and Army. He has consulted extensively in the U.S. and abroad in the areas of electromagnetics and communications. He has many published papers in the fields of antennas, microwaves, EMC, and circuit theory. He also holds two patents on TV transmitting antennas.

Optical Control of GaAs MESFET's

ALVARO AUGUSTO A. DE SALLES

Abstract—**Theoretical and experimental work for the performance of GaAs MESFET's under illumination from light of photon energy greater than the bandgap of the semiconductor is described. A simple model to estimate the effects of light on the dc and RF properties of MESFET's is presented. Photoconductive and photovoltaic effects in the active channel and substrate are considered to predict the change in the dc equivalent circuit parameters of the FET, and from these the new Y- and S-parameters under illumination are calculated. Comparisons with the measured S-parameters without and under illumination show very close agreement.**

Optical techniques can be used to control the gain of an FET amplifier and the frequency of an FET oscillator. Experimental results are presented showing that the gain of amplifiers can be varied up to around 20 dB and that the frequency of oscillators can be varied (tuning) around 10 percent when the optical absorbed power in the active region of the FET is varied by a few microwatts.

When the laser beam is amplitude-modulated to a frequency close to the free-running FET oscillation frequency, optical injection locking can occur. An analytical expression to estimate the locking range is presented. This shows a fair agreement with the experiments. Some suggestions to improve the optical locking range are presented.

I. Introduction

IN THE LAST FEW YEARS, an increasing interest has been shown on the possibilities of using the light effects to control the various functions of the FET's. Conventional methods of MESFET amplifier and oscillator control involve direct electrical connection of the control source to the device. However, in optical control, light provides the coupling medium, allowing the control signal to be distributed using optical fiber technology. This offers considerable advantages, particularly where electrical isolation and immunity from electromagnetic interference are important requirements.

The injection of light provides effectively an extra terminal to the device, which possesses inherent optical isolation, no decoupling structures being required. These decoupling structures are very often undesired because they are usually lossy and their dimensions can be unsuitable for the miniaturization required. Also, in the near infrared region (photon energies close to the GaAs bandgap) the optical absorption depths in GaAs are of the order of 1 μm, therefore being compatible with the microwave device structures.

Some experiments have shown that the FET dc characteristics may alter with illumination [1] and that FET oscillators may be tuned by varying the intensity of the light falling on the active region of the device [2]. Also, some authors [3]–[5] have recently reported high-speed optical detection with GaAs MESFET's.

The present work has been developed elsewhere [6] in more detail. Only commercially available GaAs MESFET's were used, providing therefore very poor coupling efficiency between optical and microwave energies due to the small active region available for optical absorption. However, since more and more systems are using optical transmission, direct optical interfaces become very attractive. Thus future development with a modification of the present available device structure for optimum optical/microwave interaction is likely.

The fundamental physical mechanism arising in optical illumination of the MESFET is the production of free carriers (electron-pairs) within the semiconductor material when light of photon energy equal to or greater than the semiconductor bandgap energy is absorbed. Gaps between

Manuscript received February 7, 1983; revised April 2, 1983. This work was supported in part by the U.K. Science Research Council, the U.K. Ministry of Defense (A.S.W.E.), and the CNP_q (Brasil).

The author is with Centro de Estudos em Telecommunicações (CETUC), PUC/RJ, Rua Marquês de São Vincente, 225-Rio de Janeiro-RJ, BRASIL.

0018-9480/83/1000-0812$01.00 ©1983 IEEE